

## Full color control and white emission from conjugated polymer nanofibers

Andrea Camposeo, Francesca Di Benedetto, Roberto Cingolani, and Dario Pisignano

Citation: *Applied Physics Letters* **94**, 043109 (2009); doi: 10.1063/1.3064139

View online: <http://dx.doi.org/10.1063/1.3064139>

View Table of Contents: <http://scitation.aip.org/content/aip/journal/apl/94/4?ver=pdfcov>

Published by the AIP Publishing

---

### Articles you may be interested in

[Dramatic enhancement of photo-oxidation stability of a conjugated polymer in blends with organic acceptor](#)  
*Appl. Phys. Lett.* **92**, 243311 (2008); 10.1063/1.2945801

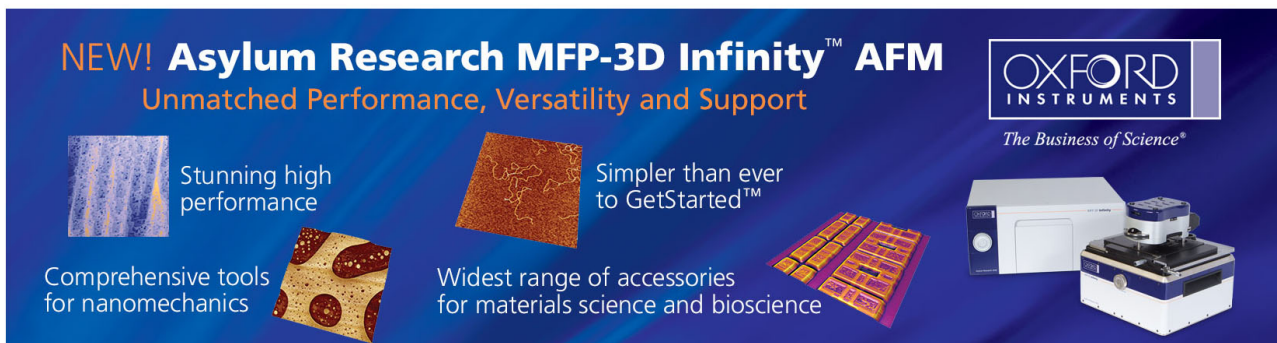
[Highly polarized luminescence from aligned conjugated polymer electrospun nanofibers](#)  
*Appl. Phys. Lett.* **92**, 213305 (2008); 10.1063/1.2936998

[Bright and efficient exciplex emission from light-emitting diodes based on hole-transporting amine derivatives and electron-transporting polyfluorenes](#)  
*J. Appl. Phys.* **91**, 10147 (2002); 10.1063/1.1481203

[Efficient polymer light-emitting diodes using conjugated polymer blends](#)  
*Appl. Phys. Lett.* **80**, 1891 (2002); 10.1063/1.1459770

[Nonlinear emission and recombination in conjugated polymer waveguides](#)  
*J. Appl. Phys.* **85**, 1124 (1999); 10.1063/1.369237

---



**NEW! Asylum Research MFP-3D Infinity™ AFM**  
Unmatched Performance, Versatility and Support

**OXFORD INSTRUMENTS**  
*The Business of Science®*

Stunning high performance

Simpler than ever to GetStarted™

Comprehensive tools for nanomechanics

Widest range of accessories for materials science and bioscience

# Full color control and white emission from conjugated polymer nanofibers

Andrea Camposeo, Francesca Di Benedetto, Roberto Cingolani, and Dario Pisignano<sup>a)</sup>  
*National Nanotechnology Laboratory (NNL) of INFM-CNR, Scuola Superiore ISUFI, Università del Salento and Italian Institute of Technology (IIT), via Arnesano, I-73100 Lecce, Italy*

(Received 24 September 2008; accepted 12 December 2008; published online 27 January 2009)

The authors demonstrate full color tunability in the visible range, including white emission, by polymer nanofibers based on binary blends of conjugated materials. The nanofibers are realized by electrospinning and their emission is based on the dipole-dipole energy transfer from a blue-emitting donor and a red-emitting acceptor conjugated polymer. The fibers are characterized by scanning electron microscopy and time-resolved and cw photoluminescence. Light emission is tuned from blue to red, including bright white with color coordinates (0.38, 0.34) according to the standard of the Commission Internationale de l'Éclairage. Polymer nanofibers based on blends of conjugated compounds turn out to be a promising class of organic semiconductor building blocks for nanophotonics. © 2009 American Institute of Physics. [DOI: 10.1063/1.3064139]

There is today a tremendous impulse toward miniaturizing the size of light-emitting sources, aiming to an effective integration with sensors and lab-on-chip devices.<sup>1-4</sup> While so far these devices have been necessarily connected to external light-emitting sources for fluorescence excitation and detection, the miniaturization of polymer light-emitting sources could open the way for the realization of truly portable devices. However, achieving tunability of nanoscale light-emitting sources remains a challenge, materials emitting at different wavelengths typically requiring specific, often expensive, and technologically demanding nanofabrication tools. For instance, to be defined at the nanoscale, bulk inorganic materials have to be processed by electron beam, x ray, or similar lithographies. White-emitting semiconducting colloidal particles<sup>5-7</sup> generally rely on hardly controllable surface-state or trap emission, whereas soft organic semiconductors are difficultly patterned at high resolution without altering their emissive properties by oxygen incorporation.

Unlike conventional approaches, electrospinning (ES) permits very high throughput, relying on the competition between applied electric field (1–50 kV voltage applied on distances of 10–50 cm) and surface tension (generally of the order of tens of mN m<sup>-1</sup>) of organic solutions.<sup>8-10</sup> The ES exploits the charged polymer ejection of a Taylor cone from a metallic needle to a whipping instability region, occurring in the range of milliseconds. The resulting plastic stretching determines a cross section reduction up to six orders of magnitude, namely, the formation of fibers of submicrometer in diameter. Recently, white emission from electrospun polymer-based nanofibers has been achieved by polyvinyl alcohol<sup>11</sup> and polystyrene<sup>12</sup> matrices embedding ZnO quantum dots<sup>11</sup> and europium complexes.<sup>12</sup> In this letter, we report on widely tunable plastic nanofibers for optoelectronics based on blends of conjugated polymers, demonstrating color tunability from blue to red including white light.

Blends of the red-emitting conjugated polymer, poly[2-methoxy-5-(2-ethylhexyloxy)-1,4-(1-cyanovinyl)phenylene] - co - [2,5-bis(N,N'-diphenylamino)-1,4-phenylene] (RE) [molecular weight

(MW)=32 000], and the blue-emitting, poly[(9,9-hexylfluorenyl-2,7-diyl)-alt-co-(9-ethyl-3,6-carbazole)] (BE) (MW=20 000) are dissolved in 5:1 (v:v) chloroform:dimethyl sulfoxide at 10% (w/v) concentration. The conjugated polymer blends are electrospun by placing a few milliliters of solution into a hypodermic syringe tipped with a 21-gauge stainless steel needle, connected to a high voltage supply (XRM30P, Gamma High Voltage Research, Inc.). The solution is injected at the end of the needle at a rate of 0.09  $\mu$ l/min by a syringe pump and the fibers are collected onto a grounded collector at a distance of 15–20 cm from the needle. All the ES experiments are performed at room temperature with air humidity of about 50% and an applied bias in the range of 18–27 kV. A scanning electron microscopy (SEM) investigation is performed using a Raith 150 electron beam system operating with an acceleration voltage in the range of 5–10 kV and an aperture size of 30  $\mu$ m, imaging samples without any conductive pre-coating. Fibers exhibit a diameter of a few hundreds of nanometers (inset in Fig. 1), with typical Gaussian diameter distributions. Beads of size around 1  $\mu$ m are observed in some samples, with a frequency of the order of one bead per 100  $\mu$ m of electrospun fibers. The photoluminescence (PL) emission of nanofiber mats deposited on quartz substrates is collected by excitation from a diode laser (energy of 3.05 eV and power <10 mW).

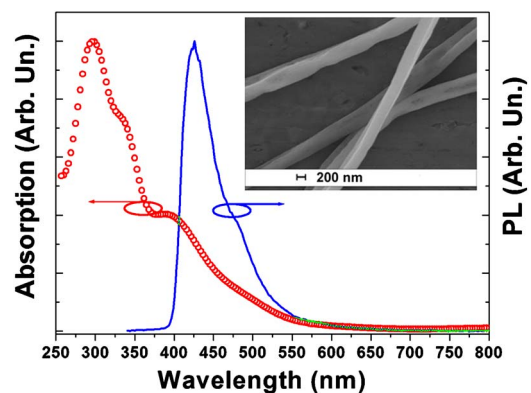


FIG. 1. (Color online) Normalized PL emission spectrum of BE (solid line, right vertical scale) and optical absorption spectrum of RE (empty circles, left scale), relevant for Förster energy transfer. Inset: SEM image of nanofibers by conjugated polymer blends.

<sup>a)</sup> Author to whom correspondence should be addressed. Electronic mail: dario.pisignano@unile.it.

The nanofiber PL at room temperature in air is collected by an optical fiber coupled to a monochromator and a charge-coupled device (CCD) detector. Time-resolved PL measurements are performed exciting the nanofiber mats by the second harmonic of a mode-locked Ti:sapphire laser delivering pulses at about 800 nm with duration of <100 fs. The PL signal is dispersed by a monochromator coupled with a streak camera (Hamamatsu) equipped with a two-dimensional CCD.

As a color tunability mechanism for the conjugated polymer nanofibers, we investigate donor-acceptor energy transfer in bicomponent samples. The BE emission and RE absorption spectra are peaked at 450 and 300 nm, respectively (dotted and solid lines in Fig. 1), such spectral superposition determining dipole-dipole energy transfer toward the vinyl-naphthylene copolymer, with values of about 4–5 nm for the Förster characteristic radius,

$$R_0 = \left[ 0.5291 \frac{\kappa^2 \eta_D}{n^4 N_{AV}} \int F_H(\nu) \sigma_D(\nu) \frac{d\nu}{\nu^4} \right]^{1/6}. \quad (1)$$

In the previous expression,  $F_H$  and  $\sigma_D$  indicate the donor emission and the acceptor molar decadic extinction coefficient, respectively,  $\eta_D$  is the BE luminescence quantum yield,  $\kappa^2$  is an orientational factor for the dipole moment distribution (of the order of unity and  $\frac{2}{3}$  for a random ensemble of dipoles in a low-viscosity medium),<sup>13</sup>  $n$  is the refractive index ( $\sim 1.7$ ),<sup>14</sup> and  $N_{AV}$  is Avogadro's number.

In the bicomponent nanofiber, the acceptor interacts with a distribution of donor chromophores dislocated along its chains, whose distance from the low-energy gap guest is limited by the effective molecular and the fiber radii. The rate of energy transfer ( $K_{ET}$ ) via point-point dipole interaction is controllable by varying the relative molar concentration of acceptors and donors (RE:BE)  $\chi$ . The resulting color is therefore effectively tailorable since the probability  $P$  of exciton transfer from the donor to the acceptor is given by  $P = K_{ET} / [(1/\tau_D) + K_{ET}]$ , where  $\tau_D$  is the BE characteristic time of spontaneous emission.<sup>15–17</sup>

The PL spectra from the bicomponent nanofibers are shown in Fig. 2(a), evidencing how concentrations as low as 1:10<sup>2</sup> still result in almost complete energy transfer to the acceptor, whereas for  $\chi < 10^{-2}$  the blue peak from the BE becomes more and more evident.  $P$ , obtained by the PL spectra from nanofibers with RE:BE relative concentrations (relative number of molecules) between 1:1 and 1:10<sup>4</sup>, and by taking into account the luminescence efficiencies of the two species [0.75 and 0.37 for BE (Ref. 17) and RE,<sup>18</sup> respectively], nonlinearly increases as  $\chi$  increases [Fig. 2(b)].

In addition, the donor decay time decreases upon including RE molecules in the nanofibers, with  $1/e$  decay times varying from 30 to 20 ps, which is a clear signature of faster excitation depopulation through energy transfer (Fig. 3).<sup>19,20</sup> On its turn, the acceptor emission exhibits a rise time ( $\sim 10$  ps), confirming that its exciton population is not directly caused by pumping photons, being instead mediated by the donor (Fig. 3).

We note that a band of emission is appreciable between 480 and 530 nm in the PL spectra from fibers with  $\chi = 10^{-2}$ ,  $10^{-3}$ , and  $10^{-4}$  [Fig. 2(a)]. The emission from these compounds typically exhibit different spectral components, deriving from the glassy ( $\alpha$ -) and from a relatively ordered ( $\beta$ -) phase, respectively. The  $\beta$ -phase, related to a planarized

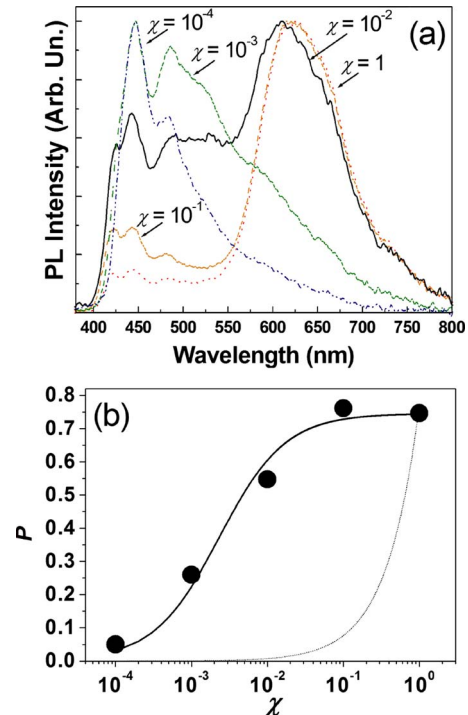


FIG. 2. (Color online) (a) PL spectra of the conjugated polymer blend nanofibers for different RE:BE relative concentrations:  $\chi=1$  (dashed curve),  $10^{-1}$  (dotted curve),  $10^{-2}$  (continuous curve),  $10^{-3}$  (dash-dotted curve), and  $10^{-4}$  (dash-dash-dotted curve). Peak wavelengths are at 625, 616, 610, 447, and 447 nm, with the full width at half maximum=107, 108, 263, 155, and 75 nm, respectively. All spectra are corrected for the instrumentation response. (b) Donor-acceptor exciton transfer probability  $P$  calculated from PL data vs  $\chi$ . For comparison, the dotted curve indicates the corresponding values of  $P$  that one would obtain assuming a linear dependence of the ratio between the emitted intensities from RE and BE on  $\chi$ . The continuous line is a guide for the eyes.

molecular configuration, results in a more extended  $\pi$ -conjugation, redshift in absorption and fluorescence spectra in the range of 100–200 meV, and narrower spectral features because of the reduced inhomogeneous and homogeneous broadening.<sup>21–23</sup> The different phases often coexist in the material, thus determining complex spectra with superimposed hardly separable emission contributions, and their relative amplitudes are strongly sensitive to the polymer pro-

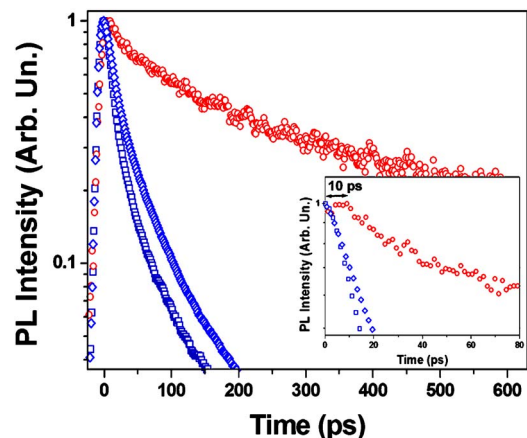


FIG. 3. (Color online) Time-resolved PL decay of BE (diamonds and squares) and RE (circles) emissions for pure BE (diamonds) and within bicomponent nanofibers (squares and circles) with  $\chi=10^{-1}$ . The horizontal dotted line marks the  $1/e$  decay times. Inset: zoom of the early decay region, evidencing the rise time of the acceptor PL with respect to the donor.



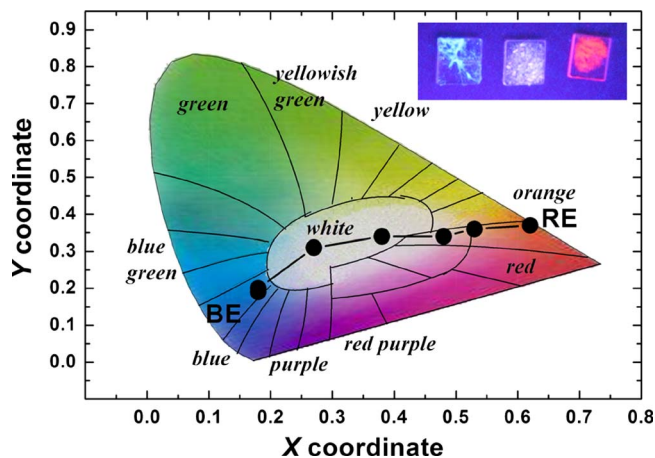


FIG. 4. (Color online) Nanofiber CIE chromaticity coordinates for different RE:BE concentrations. From right to left: pure RE,  $\chi=1$ ,  $10^{-1}$ ,  $10^{-2}$  (white emission),  $10^{-3}$ ,  $10^{-4}$ , and pure BE fibers. Inset: from left to right, photograph of blue-, white-, and red-emitting nanofibers deposited onto quartz substrates and emitting under UV cw excitation.

cessing. In addition, a low-energy band peaked at 2.2–2.3 eV is also often observable, which has been attributed to emission from excimers or aggregates,<sup>21</sup> or from on-chain defects.<sup>24–26</sup> Fluorenone-based excimers are also suggested as origin of the low-energy emission.<sup>27</sup> These phenomena can explain the low-energy tail ( $\lambda > 520$  nm), which is appreciable in the nanofiber spectra from  $10^{-3}$  to  $10^{-4}$  RE:BE relative concentrations. Furthermore, a peak at 480–485 nm is clearly appreciable in the PL of the composite fibers [Fig. 2(a)] and is largely responsible for the balanced white emission achieved at  $\chi=10^{-2}$ . We propose as possible mechanism for this feature an enhancement in the ordered phase of the BE compound with respect to the glassy one. Both the ES process, inducing a remarkable stress by the stretching due to the high applied electric field, and blending polyfluorenes with other polymers<sup>21,28</sup> can indeed determine a backbone planarization and a higher degree of order in the material. Recently, the  $\beta$ -phase was also found to exhibit a photostability enhanced by several orders of magnitude with respect to the disordered one,<sup>21</sup> and to dominate the spectrum from polyfluorenes at the solid state even if a small fraction (few percent) of the chains undergo planarization.<sup>29</sup>

An important issue for exploiting nanofibers in optoelectronic devices is their photostability in air conditions. Oxygen is indeed known to quench the fluorescence of conjugated polymers,<sup>30</sup> thus significantly reducing the quantum yield and emission lifetime. However, we cannot appreciate remarkable differences in the fibers photostability within the investigated range of  $\chi$ . Our samples preserve stability for several months under ambient storage conditions in the dark.

Furthermore, the PL spectra do not show remarkable variations with respect to the corresponding spin-cast films, with linewidth differences below 10%, and with comparable values of the emission yields. Slight blueshifts (5–8 nm) are observed in the RE peak wavelength of the nanofibers, which can be attributed to the different packing geometries induced by ES, namely, to suppression of exciton migration toward low-energy RE chromophores. Overall, the bicomponent nanofiber emission allows covering the whole visible range, including bright white (photograph in the inset of Fig. 4). The emission color, characterized according to the standard

of the Commission Internationale de l'Éclairage (CIE) as a point in two-dimensional space of coordinates ( $X, Y$ ) (Fig. 4), well matches a balanced white PL emission (0.38, 0.34) for a concentration  $\chi=10^{-2}$ .

Polymer fibers based on binary blends of conjugated compounds turn out to be a valuable class of organic semiconductor building blocks for nanophotonics. Investigating blends by different donor-acceptor systems will allow one to assess the general validity of this approach for producing white-emitting nanofibers. In this respect, the ES technology is a promising candidate for the realization of widely tunable organic nanostructures.

We gratefully acknowledge R. Stabile for the SEM and G. Morello for the time-resolved measurements.

- <sup>1</sup>X. Duan, Y. Huang, Y. Cui, J. Wang, and C. M. Lieber, *Nature (London)* **409**, 66 (2001).
- <sup>2</sup>Y. Xia, P. Yang, Y. Sun, Y. Wu, B. Mayers, B. Gates, Y. Yin, F. Kim, and H. Yan, *Adv. Mater. (Weinheim, Ger.)* **15**, 353 (2003).
- <sup>3</sup>J. M. Moran-Mirabal, J. D. Slinker, J. A. DeFranco, S. S. Verbridge, R. Ilic, S. Flores-Torres, H. Abruña, G. G. Malliaras, and H. G. Craighead, *Nano Lett.* **7**, 458 (2007).
- <sup>4</sup>F. Di Benedetto, A. Camposeo, S. Pagliara, E. Mele, L. Persano, R. Stabile, R. Cingolani, and D. Pisignano, *Nat. Nanotechnol.* **3**, 614 (2008).
- <sup>5</sup>A. A. Bol and A. Meijerink, *Phys. Chem. Chem. Phys.* **3**, 2105 (2001).
- <sup>6</sup>H. S. Chen, S. J. J. Wang, C. J. Lo, and J. Y. Chi, *Appl. Phys. Lett.* **86**, 131905 (2005).
- <sup>7</sup>M. J. Bowers II, J. R. McBride, and S. J. Rosenthal, *J. Am. Chem. Soc.* **127**, 15378 (2005).
- <sup>8</sup>D. H. Reneker and I. Chun, *Nanotechnology* **7**, 216 (1996).
- <sup>9</sup>A. G. MacDiarmid, W. E. Jones, Jr., I. D. Norris, J. Gao, A. T. Johnson, Jr., N. J. Pinto, J. Hone, B. Han, F. K. Ko, H. Okuzaki, and M. Llaguno, *Synth. Met.* **119**, 27 (2001).
- <sup>10</sup>D. Li and Y. Xia, *Adv. Mater. (Weinheim, Ger.)* **16**, 1151 (2004).
- <sup>11</sup>X. M. Sui, C. L. Shao, and Y. C. Liu, *Appl. Phys. Lett.* **87**, 113115 (2005).
- <sup>12</sup>H. Zhang, H. Song, B. Dong, L. Han, G. Pan, X. Bai, L. Fan, S. Lu, H. Zhao, and F. Wang, *J. Phys. Chem. C* **112**, 9155 (2008).
- <sup>13</sup>L. M. Herz, C. Silva, R. H. Friend, R. T. Phillips, S. Setayesh, S. Becker, D. Marsitsky, and K. Müllen, *Phys. Rev. B* **64**, 195203 (2001).
- <sup>14</sup>M. Campoy-Quiles, G. Heliotis, R. Xia, M. Ariu, M. Pintani, P. Etchegoin, and D. D. C. Bradley, *Adv. Funct. Mater.* **15**, 925 (2005).
- <sup>15</sup>T. Forster, *Ann. Phys.* **437**, 55 (1948).
- <sup>16</sup>A. K. Sheridan, A. R. Buckley, A. M. Fox, A. Bacher, D. D. C. Bradley, and I. D. W. Samuel, *J. Appl. Phys.* **92**, 6367 (2002).
- <sup>17</sup>A. Camposeo, E. Mele, L. Persano, D. Pisignano, and R. Cingolani, *Phys. Rev. B* **73**, 165201 (2006).
- <sup>18</sup>E. Mele, F. Di Benedetto, L. Persano, R. Cingolani, and D. Pisignano, *Nano Lett.* **5**, 1915 (2005).
- <sup>19</sup>A. Dogariu, R. Gupta, A. J. Heeger, and H. Wang, *Synth. Met.* **100**, 95 (1999).
- <sup>20</sup>G. Bongiovanni, C. Botta, G. Di Silvestro, M. A. Loi, A. Mura, and R. Tubino, *Chem. Phys. Lett.* **345**, 386 (2001).
- <sup>21</sup>K. Becker and J. Lupton, *J. Am. Chem. Soc.* **127**, 7306 (2005).
- <sup>22</sup>E. Conwell, *Trends Polym. Sci.* **5**, 218 (1997).
- <sup>23</sup>M. Grell, D. D. C. Bradley, G. Ungar, J. Hill, and K. S. Whitehead, *Macromolecules* **32**, 5810 (1999).
- <sup>24</sup>J. M. Lupton, M. R. Craig, and E. W. Meijer, *Appl. Phys. Lett.* **80**, 4489 (2002).
- <sup>25</sup>E. J. W. List, R. Guentner, P. Scanducci de Freitas, and U. Scherf, *Adv. Mater. (Weinheim, Ger.)* **14**, 374 (2002).
- <sup>26</sup>X. Gong, D. Moses, A. J. Heeger, and S. Xiao, *J. Phys. Chem. B* **108**, 8601 (2004).
- <sup>27</sup>M. Sims, D. D. C. Bradley, M. Ariu, M. Koeberg, A. Asimakis, M. Grell, and D. G. Lidzey, *Adv. Funct. Mater.* **14**, 1037 (2004).
- <sup>28</sup>J. A. Teetsov and D. A. Vandev Bout, *J. Am. Chem. Soc.* **123**, 3605 (2001).
- <sup>29</sup>A. L. T. Khan, P. Sreearunothai, L. M. Herz, M. J. Banach, and A. Köhler, *Phys. Rev. B* **69**, 085201 (2004).
- <sup>30</sup>M. Yan, L. J. Rothberg, F. Papadimitrakopoulos, M. E. Galvin, and T. M. Miller, *Phys. Rev. Lett.* **73**, 744 (1994).